Journal of
Materials Chemistry B

PAPER

View Article Online
View Journal | View Issue

Cite this: J. Mater. Chem. B, 2015, 3, 7427

Spatiotemporal activation of molecules within cells using silica nanoparticles responsive to blue-green light

Takaki Amamoto,[a] Tomoya Hirata,[a] Hironori Takahashi,[b] Mako Kamiya,[b] Yasuteru Urano,[abc] Tomofumi Santa[a] and Masaru Kato*[a]

Received 17th June 2015,
Accepted 11th August 2015

DOI: 10.1039/c5tb01165e

www.rsc.org/MaterialsB

The spatiotemporal control of molecular function is important but there are currently few techniques for noninvasively controlling various types of molecules in live cells. Herein we developed nanoparticles with a boron dipyrromethene structure, which are responsive to blue-green visible light. Fluorophores (fluorescein, rhodamine B, and Nile blue A) encapsulated within the nanoparticles were released by irradiation for 3 min with visible light. Nanoparticles were internalised by HeLa cells without the aid of a cell-penetrating peptide, serving as vehicles for the delivery of cargo molecules to the cytoplasm. The release and activation of encapsulated molecules by visible light irradiation demonstrate a novel method for the spatiotemporal control of molecular function that can be used to activate molecules inside the skin that cannot be reached by UV light, which has limited tissue penetration.

Introduction

Analytical techniques such as fluorescence lifetime imaging and stochastic optical reconstruction microscopy[1] have been applied to the investigation of the kinetics and localization of intracellular molecules.[2] Because the location and timing of intracellular molecule activation are precisely controlled in cells, much attention has been focused on the methods for controlling molecular function within cells by using a non-invasive external signal.[3] To date there are few general techniques that can be used for this purpose.[4–6]

Molecular activation using a non- or minimally invasive external physical stimulus such as electric current or light, temperature, and magnetic fields is of great interest in basic and applied research (for drug delivery, imaging, organic synthesis, and so on).[7,8] Light is among the most versatile types of stimuli since it is relatively safe and the timing, location, and duration of irradiation can be precisely controlled. We previously developed an ultraviolet (UV) light-cleavable monomer with a nitrobenzyl group to generate light-responsive nanoparticles in the form of a photodegradable gel that collapses upon irradiation with UV light.[9] These particles, which were used to control molecular function in cells, were restricted by encapsulation; that is, the interaction between encapsulated and outside molecules was hindered by the mesh structure of the gel. The functional capacity was recovered with the release of the molecule upon collapse of the mesh structure induced by UV irradiation. In this method, there was no requirement of specific functional groups that can form a chemical bond with the gel framework for encapsulation, since the molecule was physically trapped by the mesh;[10] moreover, there was no size limit for encapsulation since the gel mesh size could be altered by adjusting the size of the monomer.[11] Using this method, we were able to control the function of proteins, small molecules, and short interfering RNA within cells, demonstrating its wide applicability.[12,13] The collapse of the mesh structure occurred *via* the photoelimination of the nitrobenzyl group induced by irradiation with UV light (*ca.* 350 nm). However, the applicable area of this technique was limited due to the low tissue penetration of UV light.[14] Furthermore, the possibility of DNA damage is an important concern associated with the release of molecules within cells *via* UV irradiation.[15] Therefore, a technique that makes use of longer-wavelength light is desirable.

Upconversion has been used to increase the wavelength of a light source. The photoelimination reaction proceeds by the sequential absorption of two or more photons that are derived from longer-wavelength light,[16] and upconversion occurs without changes to the photocleavable group when the wavelength of light increases by two-fold or greater. However, high-powered light is required for photoelimination, which is associated with safety issues. The photoelimination reaction of 4-aryloxy boron dipyrromethene (BODIPY) derivatives upon irradiation

[a] Graduate School of Pharmaceutical Sciences, The University of Tokyo, 7-3-1 Hongo, Bunkyo-ku, Tokyo 113-0033, Japan. E-mail: masaru-kato@umin.ac.jp
[b] Graduate School of Medicine, The University of Tokyo, 7-3-1 Hongo, Bunkyo-ku, Tokyo 113-0033, Japan
[c] AMED CREST, 1-7-1 Otemachi, Chiyoda-ku, Tokyo, 100-0004, Japan

with blue-green visible light (~500 nm) has recently been reported.[17,18]

The reaction proceeds *via* photoinduced electron transfer, which induces solvolysis of the B–O bond of the positively charged aryl group.[17] Since the reaction proceeds at ambient irradiation power, photoelimination of the BODIPY structure is expected to be relatively safe. We hypothesized that visible light-responsive gel could be prepared from a monomer with a BODIPY structure instead of a nitrobenzyl group, and in this study, we developed silica nanoparticles that can be used to deliver molecules to cells and can be spatiotemporally controlled by visible light irradiation. This is the first report describing the control of various types of molecules in live cells by using nanoparticles stimulated by blue-green light.

Experimental

Chemicals

Benzaldehyde, 2,3-dichloro-5,6-dicyano-*p*-benzoquinone, *N*,*N*-diisopropylethylamine, aluminium chloride, dichloromethane (DCM), sodium sulphate, toluene, *n*-hexane, ethyl acetate, 4-hydroxybenzaldehyde, sodium cyanoborohydride, acetone, L(+)-arginine sodium chloride, rhodamine B, 4′,6-diamidino-2-phenylindole (DAPI), and methanol were purchased from Wako Pure Chemical Industries, Ltd (Osaka, Japan). 2,4-Dimethylpyrrole, boron trifluoride, 3-isocyanatopropyltriethoxysilane, dibutyltin dilaurate, cyclohexane, tetraethyl orthosilicate (TEOS), and potassium carbonate were from Tokyo Chemical Industry Co., Ltd (Tokyo, Japan). Silica gel 60 N (spherical, neutral) was from Kanto Chemical Co. ING. (Tokyo, Japan). Fluorescein sodium salt and fluorescein isothiocyanate (FITC)-dextran (average M_W: 20 000) were from Sigma-Aldrich (St. Louis, MO, USA). Nile blue A was from Alfa Aesar (Lancashire, UK).

Preparation of a BODIPY-based photocleavable monomer

The preparation of photocleavable monomer is outlined in Scheme 1. Benzaldehyde (256 mg) and 2,4-dimethylpyrrole (427 mg) were dissolved in 300 ml of DCM. Three drops of trifluoroacetic acid were added and the mixture was stirred for 20 h at room temperature. 2,3-Dichloro-5,6-dicyanobenzoquinone (720 mg) was added to the reaction solution, followed by stirring for 10 min at room temperature. The reaction was washed twice with water and brine and dried over Na_2SO_4. The crude product was purified by column chromatography over silica gel and the DCM fraction was evaporated under reduced pressure. The obtained solid was dissolved in 120 ml of toluene, followed by the dropwise addition of 2.4 ml of *N*,*N*-diisopropylethylamine and 3.0 ml of boron trifluoride. The solution was stirred for 2 h at room temperature under a nitrogen atmosphere, washed twice with water and brine, and purified by column chromatography over a silica gel (*n*-hexane : ethyl acetate = 3 : 1). The yield for product **1** was 41% (324 mg).[19]

The reaction product (324 mg of **1**) along with 66.7 mg of aluminium chloride was dissolved in 30 ml of DCM and refluxed at 55 °C for 5 min under an argon atmosphere. 4-Hydroxybenzaldehyde (266 mg) in 20 ml of DCM was added to the reaction using a syringe, and the solution was refluxed for 5 min. The reactant was purified using an alumina filtrate column followed by column chromatography over a silica gel (*n*-hexane : ethyl acetate = 3 : 1), then dried using an evaporator. The yield for product **2** was 42% (220 mg); this was dissolved in 40 ml of methanol, to which sodium borohydride (63 mg in 10 ml of methanol) was added using a syringe, followed by stirring for 5 min at room temperature under a nitrogen atmosphere. After adding 1 ml of acetone, the crude product was purified by column chromatography over silica gel (*n*-hexane : ethyl acetate = 1 : 1), yielding 140 mg of product **3** (63%). This was dissolved in 30 ml of ethyl acetate with stirring under a nitrogen atmosphere. 3-Isocyanatopropyltriethoxysilane

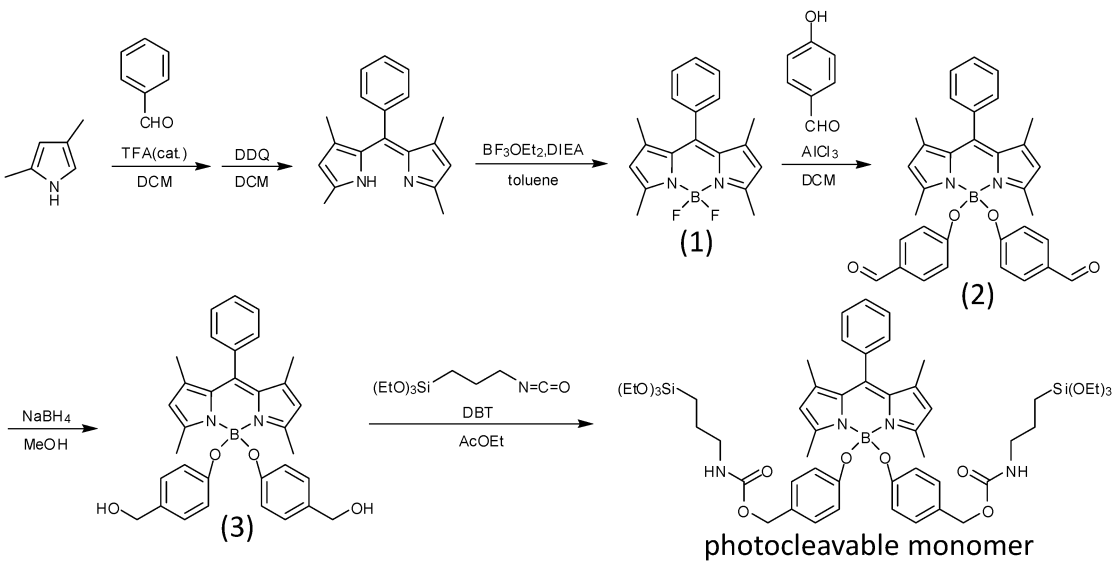

Scheme 1 Preparation of the photocleavable monomer containing a BODIPY structure.

(193 mg) and dibutyltin dilaurate (16 mg) were added to the reaction with stirring at 75 °C for 48 h. The crude product was purified by column chromatography over silica gel (*n*-hexane : ethyl acetate = 3 : 1, 10% [w/w] potassium carbonate). The yield for the photocleavable monomer was 59% (160 mg).

^{1}H NMR (500 M Hz, $CDCl_3$): δ = 7.51 (t, aromatic–*H*), δ = 7.09 (d, aromatic–*H*), δ = 7.09 (d, aromatic–*H*), δ = 6.62 (t, aromatic–*H*), δ = 5.87 (s, aromatic–*H*), δ = 4.96 (s, aromatic–CH_2O), δ = 3.8 (m, Si(OCH_2CH$_3$)$_3$), δ = 3.18 (t, NHCH_2CH$_2$), δ = 2.49 (s, aromatic–CH_3), δ = 2.05 (s, aromatic–CH_3), δ = 1.62 (m, CH$_2$CH_2CH$_2$), δ = 1.25 (t, Si(OCH$_2$CH_3)$_3$), δ = 0.61 (t, CH$_2$CH_2Si).

Preparation of visible light-responsive nanoparticles

Preparation of the seed and visible light-responsive nanoparticles. The seed and nanoparticles were prepared based on a previously described method.[20] Briefly, 9.1 mg of arginine were dissolved in 6.9 ml of water, followed by the addition of 0.45 ml of cyclohexane and 0.55 ml of TEOS in this order. The solution was stirred at 60 °C for 20 h to obtain seeds of uniform size.

A solution of 50 μl of seed, 0.5 mg of arginine, 25 μl of ethyl acetate, 20 μl of TEOS, 0.5 mg of photocleavable monomer, and 10 μl of encapsulated molecules (10 mg ml^{-1} fluorescein sodium salt, rhodamine B, Nile blue A, or FITC-dextran, 1 mg ml^{-1} DAPI) were added to 1 ml of water. The mixture was stirred overnight at 500 rpm and 60 °C. The prepared nanoparticles were purified by dialysis (Spectra/Por 6, MW cutoff: 50 000; Spectrum Laboratories, Inc., Compton, CA, USA) for 24 h to remove excess molecules that were not encapsulated by the nanoparticles.

Surface modification of nanoparticles with R8

A 150 μl volume of nanoparticle solution and 150 μl of R8 peptide (4 μM in water) were mixed and vortexed for 20 min at room temperature.

Transmission electron microscopy (TEM) measurements

TEM images were obtained using an H-7000 electron microscope (Hitachi, Tokyo, Japan) operating at 75 kV. Copper grids (400 mesh) were coated with a thin film of collodion followed by carbon. The nanoparticle dispersion (5 μl) was placed on the coated copper grids and dried at room temperature before observation.

Dynamic light scattering (DLS) measurements

A Nanotrac Wave DLS instrument (Microtrac BEL Corp., Osaka, Japan) was used to measure the diameters of the nanoparticles. Measurements were carried out at room temperature using a 780 nm laser beam. At least three replications were performed for each sample. A sample solution of 20 μl was used for measurement. Size distribution graphs of the relative intensity of scattered light with respect to the hydrodynamic diameter of nanoparticles were obtained.

Zeta potential

The nanoparticle solution was diluted 10-fold with 10 mM NaCl solution prior to the measurement of zeta potential, which was carried out on a Delsa Nano C instrument (Beckman Coulter, Inc., Brea, CA, USA).

Irradiation conditions

A halogen lamp (LG-PS2; Olympus, Tokyo, Japan) was used as a light source. The light was filtered with 500 nm band pass filters (Edmund Optics Inc., Tokyo, Japan) and used to irradiate the nanoparticle solution for 3 min at a power of 7 mW cm^{-2} (at 500 nm).

Evaluation of the release efficiency of encapsulated molecules from nanoparticles by visible light stimulation

After irradiation, the nanoparticle solution was concentrated by ultracentrifugation (Optima TLX; Beckman Coulter) at 57 000 × *g* for 10 min. The supernatant (100 μl) was poured into the wells of a 96-well micro-assay plate (BD Biosciences, Franklin Lakes, NJ, USA). The fluorescence intensity of the supernatant was measured using a multiplate reader (SH-9000; Corona Electric Co., Ibaraki, Japan). Excitation/emission wavelengths were 491/521 nm for fluorescein, 540/580 nm for rhodamine B, and 635/675 nm for Nile blue A.

Cell culture

HeLa cells were cultured in a humidified atmosphere of 95% air and 5% CO_2 at 37 °C in Dulbecco's Modified Eagle's Medium (DMEM, Sigma-Aldrich) supplemented with 1% (v/v) penicillin–streptomycin solution (100×) (Wako Pure Chemical Industries, Ltd) and 10% (v/v) foetal bovine serum (FBS; Invitrogen). For each experiment, cells at 80–90% confluence were harvested by digestion with trypsin/EDTA (Wako Pure Chemical Industries, Ltd), then washed and resuspended in fresh growth medium with FBS at a concentration of 10^6 viable cells/culture flask (75 cm^2).

Internalisation of the nanoparticles by cells

Cells in the culture dish were washed with DMEM without serum and 2 ml of DMEM were added. A 200 μl volume of as prepared nanoparticle solution was added dropwise to the dish; after allowing 1 h for internalisation, the dish was washed three times with culture medium; after incubation, the internalisation of nanoparticles was evaluated from fluorescence images.

Confocal laser scanning microscopy

Images of the cells were obtained using an LSM510 microscope (Carl Zeiss AG, Oberkochen, Germany) using a W-PI 10×/23 eyepiece (Carl Zeiss AG) and a C-Apochromat 40×/1.2W UV-VIS-NIR objective lens (Carl Zeiss AG) or using an Fv10i microscope (Olympus).

Results and discussion

Visible light-responsive nanoparticle generation and characterisation

We first prepared seed nanoparticles from tetraethyl orthosilicate (TEOS) and modified their surface with a photocleavable monomer and TEOS to generate visible light-responsive nanoparticles (Fig. 1), which was similar to the procedure used to prepare UV-responsive nanoparticles described in our previous report.[9c]

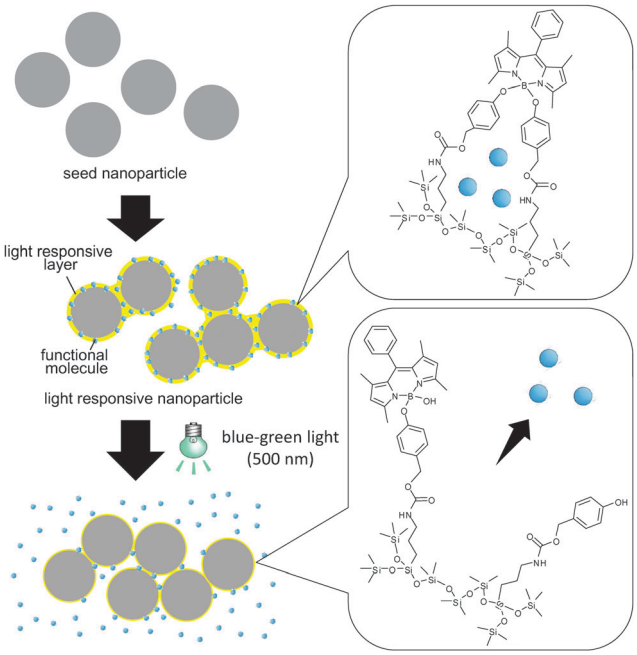

Fig. 1 Schematic illustration of light-responsive nanoparticles and photocleavage reaction of the BODIPY structure.

DLS measurements indicated that the average sizes of the seed and functional nanoparticles were 25 and 70 nm, respectively (Fig. 2a). A TEM analysis revealed that seed particles were monodispersed and had globular form, whereas BODIPY nanoparticles formed clusters without significant changes in the nanoparticle size (Fig. 2b). Thus, the increase in the nanoparticle size by modification with the cleavable monomer was mainly due to clustering and not an increase in the size of individual nanoparticles. In fact, the grey structures observed between bound nanoparticles suggested that the monomer functioned as glue. In contrast, in the case of UV-responsive nanoparticles containing a nitrobenzyl moiety as the photocleavable group,[9c] individual nanoparticles were observed to become enlarged despite being prepared under the same conditions as visible light-responsive nanoparticles. This difference may be attributed to the hydrophobicity of the BODIPY structure, which hindered the dispersion of nanoparticles in an aqueous solution.

The irradiation time for the release of encapsulated molecules was set at 20 s using a light-emitting diode (60–100 mW at 350 nm) for UV-responsive nanoparticles. Visible light-responsive nanoparticles were irradiated for a longer time (3 min) using a halogen lamp (7 mW cm^{-2} at 500 nm) for an irradiation strength that was the same as that used in our previous study.[9c] Visible light irradiation increased the average nanoparticle size to 300 nm as determined by DLS, with more clusters observed by TEM analysis, suggesting that irradiation caused alterations in the nanoparticle surface properties that consequently accelerated cluster formation. TEM results indicated that the grey colour of the structure between bound nanoparticles became lighter by irradiation, which was likely due to the cleavage reaction of the photoresponsive layer. Since the size of each nanoparticle was similar to that of the seed nanoparticle, the photoresponsive layer was presumed to form a thin surface on the nanoparticle (Fig. 1).

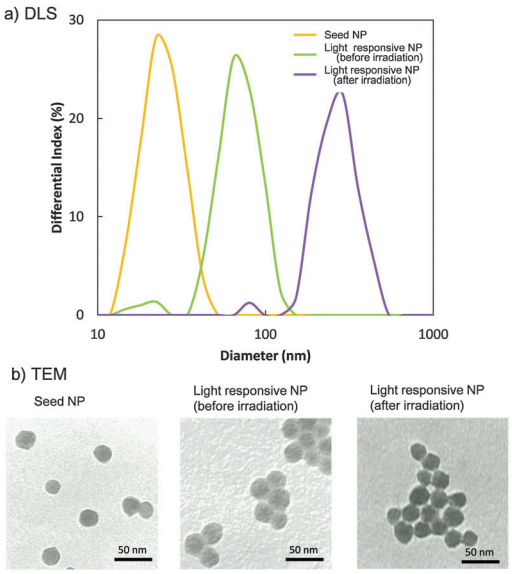

Fig. 2 (a) DLS and (b) TEM analyses of the seed nanoparticle (NP) and visible light-responsive NPs before and after irradiation.

Release and activation of encapsulated molecules by visible light

Nanoparticles with fluorophores in the outer shell were prepared by combining the photocleavable monomer TEOS and a fluorophore in a dispersed solution of seed nanoparticles (Fig. 1). We compared the fluorescence intensity of the supernatant before and after irradiation to evaluate the amount of fluorophore released upon visible light stimulation. Fluorescein, rhodamine B, and Nile blue A were selected as representative fluorophores and irradiation time was set to 3 min. Although photobleaching of organic fluorescent dyes by long exposure times has been reported,[21] the fluorescence intensities of the three fluorophores were similar before and after 3 min (7 mW cm^{-2}) of irradiation (Table 1), indicating that this exposure time did not induce photobleaching and confirming the low risk of damage associated with blue-green light. In fact, the fluorescence intensity of the supernatants of the three nanoparticle solutions was increased by irradiation (Fig. 3), indicating that the fluorophores were released as a result of changes to the nanoparticles induced by irradiation. Low fluorescence was observed in the supernatants of the three unirradiated nanoparticle solutions, which may have resulted from nanoparticles leaching during ultracentrifugation (57 000 × g for 10 min). Only a slight increase in fluorescence intensity was observed for the fluorescein-containing nanoparticle, likely because it was not retained by the negatively charged silica nanoparticle owing to electrostatic

Table 1 Ratio of fluorescence intensity before and after irradiation

Fluorophore	Fluorescein	Rhodamine B	Nile blue A
Ratio before and after irradiation	104 ± 2	100 ± 1	97 ± 2

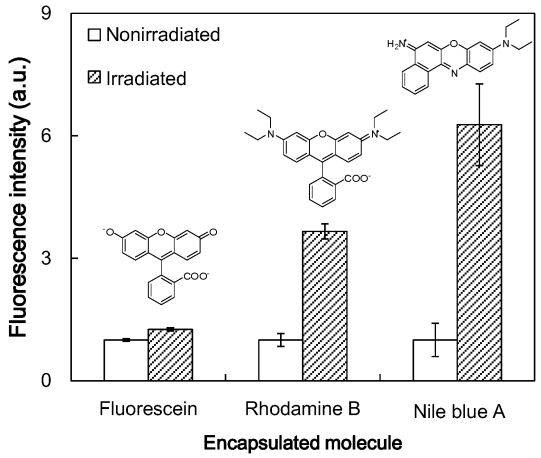

Fig. 3 Amount of fluorophore released from nanoparticles upon irradiation with blue-green visible light.

repulsion. In contrast, the fluorescence intensities of the supernatant of the rhodamine B- and Nile blue A-containing nanoparticles increased by about 4- and 6-fold, respectively, upon irradiation. This was similar to the increase observed for the UV-responsive nanoparticles that we previously investigated.[9c] There was no observable difference in the release properties, although the monomer cleavage group was changed from a nitrobenzyl to a BODIPY group.

Cell internalisation of visible light-responsive nanoparticles

We investigated whether the nanoparticle could be internalised by cells and thus serve as a molecular carrier. Rhodamine B and FITC-dextran were used as the encapsulated fluorophores. Fluorophore only, fluorophore-containing nanoparticles, and octaarginine (R8)-modified fluorophore-containing nanoparticles were added to HeLa cell culture dishes, and after washing, the fluorescence intensity of the cells was measured (Fig. 4). The fluorescence intensity of the each solution was aligned. R8 is a cell-penetrating peptide (CPP) that enhances the permeation of the cell membrane.[22] There was weak fluorescence detected in cells treated with rhodamine B and none in cells treated with FITC-dextran, indicating that the latter does not penetrate the cell membrane. However, fluorescence was observed in cells treated with fluorophore-containing nanoparticles, both with and without R8. This suggests that the nanoparticles facilitated the internalisation of the fluorophore. There was no obvious difference between nanoparticles with and without CPP modification (Fig. 4d). Thus, the developed nanoparticles can be taken up by cells without requiring surface modification.

To examine the mechanistic basis for the internalisation, the zeta potential of the nanoparticles was determined. The zeta potentials of the seed, unmodified, and R8-modified nanoparticles were −14, −1, and 7 mV, respectively. Although the seed was originally negatively charged, the charge was effectively neutralized by modification with the photocleavable monomer, and became positive by additional modification with R8. The polarity change of the nanoparticles' zeta potential likely reduced electrostatic repulsion from the negatively charged cellular membrane thereby accelerating their

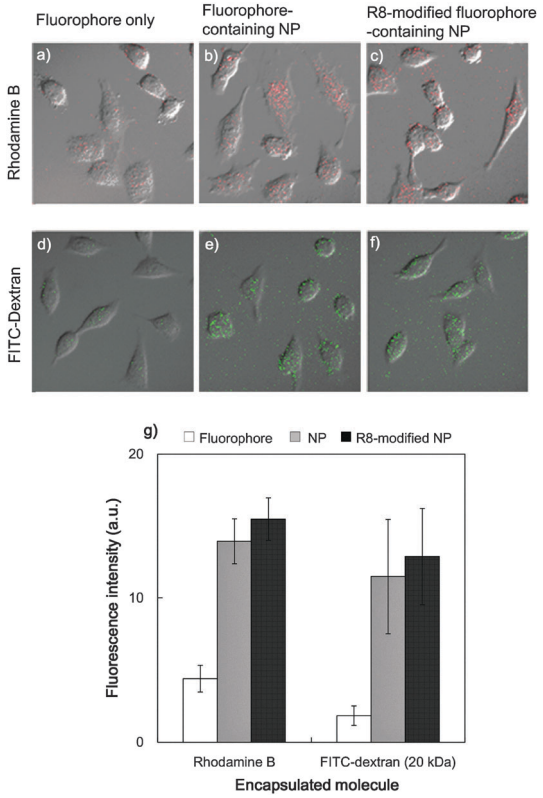

Fig. 4 Confocal laser scanning micrographs of HeLa cells treated with (a) rhodamine B, (b) rhodamine B-containing nanoparticles, (c) R8-modified rhodamine B-containing nanoparticles, (d) FITC-dextran, (e) FITC-dextran-containing nanoparticles, and (f) R8-modified FITC-dextran-containing nanoparticles. (g) Comparison of fluorescence intensity of cells treated with fluorophore and nanoparticles.

internalisation. The change in zeta potential to a positive value also confirmed the modification of the nanoparticle surface with R8, although this did not significantly improve internalisation efficiency. These results indicate that the light-responsive nanoparticles are an effective vehicle for the delivery of cargo molecules into cells.

Spatiotemporal release and activation of cargo molecules within cells by visible light

To determine whether the nanoparticles can function as photoactivatable carriers, we examined the release of cargo molecules within cells upon irradiation. DAPI was chosen as a cargo molecule, since its fluorescence intensity is increased about 20-fold by complex formation with DNA.[23] There was almost no fluorescence observed in cells that internalised DAPI-containing nanoparticles (Fig. 5a). This is because the DAPI molecule was encapsulated within the nanoparticle mesh structure, which hindered the interactions with DNA. In contrast, strong fluorescence was observed throughout the cells upon irradiation for 3 min (7 mW cm^{-2}, Fig. 5b and d), presumably because encapsulated DAPI was released and formed complexes with DNA. This indicated that internalised nanoparticles were not exocytosed by cells, but instead escaped

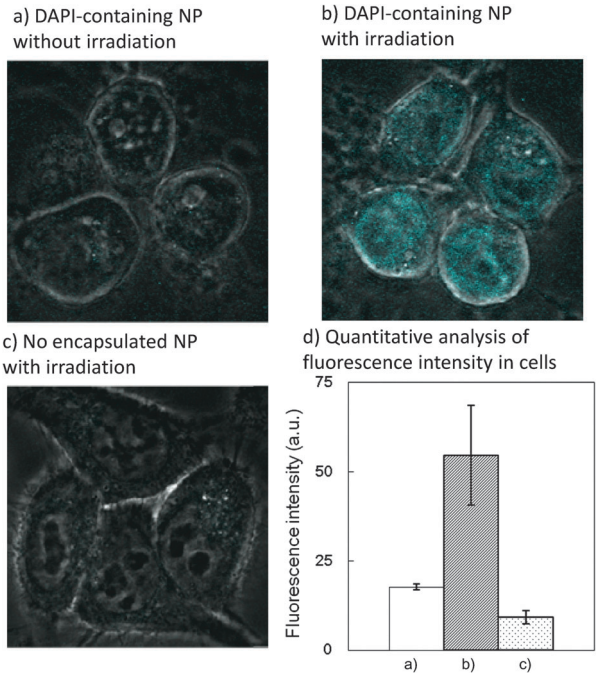

Fig. 5 (a–c) Confocal laser scanning micrographs of HeLa cells treated with DAPI-containing nanoparticles (NPs) with (a) and without (b) visible light irradiation and no encapsulated nanoparticles with irradiation (c). (d) Quantitative analysis of fluorescence intensity.

from the endosome and remained in the cytoplasm. The release of DAPI from nanoparticles and its subsequent distribution throughout the cell occurred rapidly. The fluorescence intensity was higher in the nucleus than in the cytoplasm, suggesting that DAPI diffused freely and was concentrated in the nucleus where most cellular DNA is localised. The fluorescence was not observed in cells that internalised non-encapsulated nanoparticles with 3 min irradiation (Fig. 5c). These results indicate that the spatiotemporal release within the cells of molecules carried by the nanoparticles can be controlled by visible light.

Conclusions

We developed a BODIPY-derivatised monomer that was used to prepare visible light-responsive nanoparticles. These were internalised by cells without requiring surface modifications such as a CPP and were induced to release cargo molecules by irradiation with visible light. Although various light-responsive nanoparticles have been developed to date, most respond only to UV light. We expect that these light-responsive nanoparticles can be more effective carriers of cargo molecules in deep tissues that cannot be penetrated by UV light.

Acknowledgements

We thank Dr S. Fukuda (U. Tokyo) and Dr N. Kaji (Nagoya Univ.) for technical assistance with TEM measurements and in donating the R8 peptide, respectively. This work was supported by grants (Kakenhi) from the Ministry of Education, Culture, Sports, Science, and Technology (MEXT) of Japan and JSPS Core-to-Core Program, A. Advanced Research Networks.

Notes and references

1 (*a*) H. T. T. Duong, F. Hughes, S. Sagnella, M. Kavallaris, A. Macmillan, R. Whan, J. Hook, T. P. Davi and C. Boyer, *Mol. Pharmceutics*, 2012, **9**, 3046–3061; (*b*) J. S. Basuki, H. T. T. Duong, A. Macmillan, R. B. Erlich, L. Esser, M. C. Akerfeldt, R. M. Whan, M. Kavallaris, C. Boyer and T. P. Davis, *ACS Nano*, 2013, **7**, 10175–10189; (*c*) F. Kurniawansyah, H. T. T. Duong, L. T. Danh, R. Mammucari, O. Vittorio, C. Boyer and N. Foster, *Chem. Eng.*, 2015, **279**, 799–808; (*d*) A. E. Dunn, D. J. Dunn, A. Macmillan, R. Whan, T. Stait-Gardner, W. S. Price, M. Lim and C. Boyer, *Polym. Chem.*, 2014, **5**, 3311–3315; (*e*) M. J. Rust, M. Bates and X. Zhuang, *Nat. Methods*, 2006, **3**, 793–796; (*f*) B. Huang, W. Q. Wang, M. Bates and X. W. Zhuang, *Science*, 2008, **319**, 810–813.

2 E. Kuranaga and M. Miura, *Trends Cell Biol.*, 2007, **17**, 135–144.

3 M. Kato, *Bunseki Kagaku*, 2015, **64**, 77–87.

4 K. Deisseroth, G. Feng, A. K. Majewska, G. Miesenböck, A. Ting and M. J. Schnitzer, *J. Neurosci.*, 2006, **26**, 10380–10386.

5 G. Mayer and A. Heckel, *Angew. Chem., Int. Ed.*, 2006, **45**, 4900–4921.

6 K. R. Thomas, K. R. Folger and M. R. Capecchi, *Cell*, 1986, **44**, 419–428.

7 J. Xu, K. Jung, A. Atme, S. Shanmugam and C. Boyer, *J. Am. Chem. Soc.*, 2014, **136**, 5508–5519.

8 (*a*) S. A. Hoffman and S. P. Stayton, *Macromol. Symp.*, 2004, **207**, 139–151; (*b*) J. Ge, E. Neofytou, T. J. Cahill, R. E. Beygui and R. N. Zare, *ACS Nano*, 2012, **6**, 227–233; (*c*) M. A. C. Stuart, W. T. S. Huck, J. Genzer, M. Müller, C. Ober, M. Stamm, G. B. Sukhorukov, I. Szleifer, V. V. Tsukruk, M. Urban, F. Winnik, S. Zauscher, I. Luzinov and S. Minko, *Nat. Mater.*, 2010, **9**, 101–113; (*d*) A. P. Esser-Kahn, S. A. Odom, N. R. Sottos, S. R. White and J. S. Moore, *Macromolecules*, 2011, **44**, 5539–5553.

9 (*a*) S. Murayama and M. Kato, *Anal. Chem.*, 2010, **82**, 2186–2191; (*b*) S. Murayama, F. Ishizuka, K. Takagi, H. Inoda, A. Sano, T. Santa and M. Kato, *Anal. Chem.*, 2012, **84**, 1374–1379; (*c*) F. Ishizuka, X. S. Liu, S. Murayama, T. Santa and M. Kato, *J. Mater. Chem. B*, 2014, **2**, 4153–4158.

10 Y. Shibata, T. Santa and M. Kato, *RSC Adv.*, 2015, **5**, 65909–65912.

11 (*a*) T. Amamoto, T. Santa and M. Kato, *Chem. Pharm. Bull.*, 2014, **62**, 649–653; (*b*) K. Takagi, S. Murayama, T. Sakai, M. Asai, T. Santa and M. Kato, *Soft Matter*, 2014, **10**, 3553–3559.

12 S. Murayama, B. Su, K. Okabe, A. Kishimura, K. Osada, M. Miura, T. Funatsu, K. Kataoka and M. Kato, *Chem. Commun.*, 2012, **48**, 8380–8382.

13 (*a*) S. Murayama, T. Nishiyama, K. Takagi, F. Ishizuka, T. Santa and M. Kato, *Chem. Commun.*, 2012, **48**, 11461–11463; (*b*) S. Murayama, P. Kos, K. Miyata, K. Kataoka, E. Wagner and M. Kato, *Macromol. Biosci.*, 2014, **14**, 626–631.

14 A. M. Smith, M. C. Mancini and S. Nie, *Nat. Nanotechnol.*, 2009, **4**, 710–711.
15 R. P. Crefcoeur, R. Yin, R. Ulm and T. D. Halazonetis, *Nat. Commun.*, 2013, **4**, 1779.
16 (*a*) B. Yan, J. C. Boyer, N. R. Branda and Y. Zhao, *J. Am. Chem. Soc.*, 2011, **133**, 19714–19717; (*b*) B. Yan, J. C. Boyer, D. Habault, N. R. Branda and Y. Zhao, *J. Am. Chem. Soc.*, 2012, **134**, 16558–16561.
17 N. Umeda, H. Takahashi, M. Kamiya, T. Ueno, T. Komatsu, T. Terai, K. Hanaoka, T. Nagano and Y. Urano, *ACS Chem. Biol.*, 2014, **9**, 2242–2246.
18 (*a*) P. P. Goswami, A. Syed, C. L. Beck, T. R. Albright, K. M. Mahoney, R. Unash, E. A. Smith and A. H. Winter, *J. Am. Chem. Soc.*, 2015, **137**, 3783–3786; (*b*) N. Rubinstein, P. Liu, E. W. Miller and R. Weinstain, *Chem. Commun.*, 2015, **51**, 6369–6372.
19 T. Nagano, Y. Urano and N. Umeda, Caged compound. PCT/JP/2009/052027, February 6, 2009.
20 N. Itoh, A. Sano, T. Santa and M. Kato, *Analyst*, 2014, **139**, 4453–4457.
21 Q. Zheng, M. F. Juette, S. Jockusch, M. R. Wasserman, Z. Zhou, R. B. Altman and S. C. Blanchard, *Chem. Soc. Rev.*, 2014, **43**, 1044–1056.
22 H. Akita, R. Ito, I. A. Khalil, S. Futaki and H. Harashima, *Mol. Ther.*, 2004, **9**, 443–451.
23 B. Chazotte, *Cold Spring Harb Protoc.*, 2011, DOI: 10.1101/pdb.prot5556.